Published in final edited form as:

Nature. 2017 April 20; 544(7650): 362–366. doi:10.1038/nature22044.

Antisense oligonucleotide therapy for spinocerebellar ataxia type 2

Daniel R. Scoles[1,*], **Pratap Meera**[2], **Matthew Schneider**[1], **Sharan Paul**[1], **Warunee Dansithong**[1], **Karla P. Figueroa**[1], **Gene Hung**[3], **Frank Rigo**[3], **C. Frank Bennett**[3], **Thomas S. Otis**[2,†], and **Stefan M. Pulst**[1,*]

[1]Department of Neurology, University of Utah, 175 North Medical Drive East, 5th Floor, Salt Lake City, UT 84132, USA.

[2]Department of Neurobiology, University of California Los Angeles, Los Angeles, CA 90095, USA.

[3]Ionis Pharmaceuticals, 2855 Gazelle Court, Carlsbad, CA 92010, USA

Abstract

Adult human neurodegenerative diseases have no disease-modifying treatments. We used spinocerebellar ataxia type 2 (SCA2), an autosomal dominant polyglutamine disease1, as a model to test RNA-targeted therapies[2] in two SCA2 mouse models. Both models recreate progressive adult-onset dysfunction and degeneration of a neuronal network including decreased firing frequency of cerebellar Purkinje cells (PCs) and decline in motor function[3,4]. We developed a potential therapy directed at the *ATXN2* gene by screening 152 antisense oligonucleotides (ASOs). Here we show that the most promising lead, ASO7, downregulated *ATXN2* mRNA and protein resulting in delayed onset of SCA2 phenotypes. After delivery by intracerebroventricular injection (ICV) to ATXN2-Q127 mice, ASO7 localized to PCs, reduced cerebellar *ATXN2* expression below 75% for >10 weeks without microglial activation, and reduced cerebellar ataxin-2 protein. ASO7 treatment of symptomatic mice improved motor functioning compared to saline-treated mice. ASO7 had a similar effect in the BAC-Q72 SCA2 mouse model, and in both mouse models it normalized protein levels of several SCA2-related PC proteins including Rgs8, Pcp2, Pcp4, Homer3, Cep76, and Fam107b. Most surprisingly, firing frequency of PCs returned to

[*]Correspondence and requests for materials should be addressed to D.R.S. (Daniel.Scoles@hsc.utah.edu) or S.M.P. (Stefan.Pulst@hsc.utah.edu).

[†]Present address: Roche Pharma Research and Early Development, Neuroscience, Ophthalmology, & Rare Diseases, Roche Innovation Center Basel Grenzacherstrasse 124, CH-4070, Basel, Switzerland.

Author Contributions

D.R.S. conceived and designed the study, performed experiments, conducted all ICV injections, analyzed all data, and wrote the manuscript. M.S. performed all motor testing experiments and with D.R.S. contributed to blinding of all mouse trials including ASO treatments, motor testing and electrophysiological evaluations. M.S. also conducted all qPCR analyses of mouse tissues. P.M. designed and performed all electrophysiological experiments, analyzed and interpreted the resulting data, and prepared figures. S.P. prepared all Western blots. W.D. conducted the study of SCA2 patient fibroblasts. K.P.F. was in charge of mouse breeding. G.H. led the ASO in silico design, ASO in vitro screening, advised the in vivo screening approach, and provided ASO powders. F.R., and C.F.B. contributed to the in vivo screening approach and design of motor phenotype studies. T.S.O. designed and helped interpret the electrophysiological analyses. S.M.P. conceived and designed the study with D.R.S. and contributed SCA2 patient fibroblasts. All authors contributed to the writing of the manuscript.

The authors declare no competing financial interests. S.M.P. is a consultant for Progenitor Life Sciences and Ataxion Pharmaceuticals. T.S.O. is an employee of F. Hoffmann-La Roche, Ltd. G.H., F.R., and C.F.B are employed by Ionis Pharmaceuticals, which supplied the ASOs used in the study.

normal even when treatment was initiated >12 weeks after motor phenotype onset in BAC-Q72 mice. These findings support ASOs as a promising approach for treating some human neurodegenerative diseases.

SCA2 is caused by DNA CAG repeat expansion leading to an increase in the polyglutamine (polyQ) domain in the N-terminal part of the ATXN2 protein. Although the disease was initially described as a cerebellar degeneration, it is now known to involve multiple neuronal subtypes outside the cerebellum including presentation as amyotrophic lateral sclerosis (ALS) or Parkinson disease[5,6]. Neurodegenerative diseases caused by dominant mutations in human genes have been difficult to approach therapeutically, and few studies have targeted disease genes directly as the first step in pathogenesis (discussed below). Developing therapeutics for SCAs can be complicated by the occurrence of repeat-associated non-AUG translation (RAN) translation, which appears to be irrelevant for SCA2[7]. Although targeting the mutation itself appears attractive, this approach has proven to be technically difficult in polyQ diseases. We have used SCA2 as a model to develop an approach to use ASOs to directly target *ATXN2* mRNA.

ASOs have undergone significant recent development[2]. Modification of DNA backbone chemistry has reduced toxicity, increased target engagement, and improved destruction of DNA-RNA hybrids. We designed multiple chimeric 2'-*O*-methoxyethyl (MOE)/DNA gapmer ASOs targeting *ATXN2* for an *in vitro* screen and screened for *ATXN2* RNA reduction in a cell based assay, identifying several ASOs that reduced *ATXN2* expression. After testing of ASOs for *in vivo* tolerability, we tested one ASO in detailed behavioral, biochemical and physiological studies. This ASO targets exon 11 of human *ATXN2* and is designated ASO7.

Prior studies indicated that dosage of the polyQ expanded ATXN2 is important in pathology as homozygote animals developed more severe disease manifestations[8]. On the other hand, reducing *ATXN2* dosage did not affect survival or CNS morphology in heterozygous or homozygous knock-out animals[9], suggesting *ATXN2* reduction by ASOs as a viable strategy for SCA2-mediated neurodegeneration.

Our *in vitro* screen included 152 ASOs designed *in silico* for targeting human *ATXN2*. The top 8 lead ASOs lowered *ATXN2* expression by ≥85% (Extended Data Fig. 1, Supplementary Table 1). *In vivo* testing revealed ASO7 and two other ASOs among the most effective for lowering *ATXN2* expression after 7 d treatment (Extended Data Fig. 2a–c). To assess astroglial and microglial activation we measured cerebellar *Gfap* and *Aif1* expression by qPCR. We tested several doses of ASO7 and observed significant reduction of *ATXN2* in cerebella after 14 days treatment with 210 μg ASO7 without activation of Gfap or Aif1 (Extended Data Fig. 2a–c, and 3). Some ASOs were not further pursued owing to activation of astroglial or microglial responses in > 10 wk treatments. We verified that ASO7 as well as other lead ASOs were taken up by PCs by IHC (Extended Data Fig. 2d, e–i).

ATXN2-Q127 mice have a human *ATXN2* cDNA transgene with 127 CAG repeats. We treated ATXN2-Q127 mice ICV at 8 wks of age, coinciding with the age of motor phenotype onset[4], with ASO7 and tested motor performance on the accelerating rotarod at weeks 5, 9,

and 13 after ICV injection. Consensus criteria for the conduct of preclinical trials were closely followed (see Supplementary Discussion). Progression of motor dysfunction in saline treated mice was as previously observed[4]. Mice injected with ASO7 had significantly improved motor performance compared to saline-treated control mice (Fig. 1a), and human *ATXN2* and mouse *Atxn2* mRNA expression was reduced by 75% and 20%, respectively, after motor phenotype testing demonstrating target engagement (Fig. 2a–c).

In preclinical studies, it is important to test compounds in multiple models of the human disease. We therefore developed a mouse model that replicated the human disease more closely by expressing a bacterial-artificial-chromosome (BAC) transgene incorporating the human promoter as well as all exons and introns and flanking regions. The BAC resulted in expression of ATXN2 with 72 glutamines in multiple neuronal tissues including spinal cord[3]. The BAC-Q72 model approximates human disease not only with regard to disease manifestations and less dramatic progression, but also because it contains the entire human gene in its proper intronic-exonic context. We conducted an additional preclinical trial in this mouse model with treatment initiated at 8 wks of age, as for the experiment using ATXN2-Q127 mice. Again, the mutated human *ATXN2* and mouse *Atxn2* were engaged by ASO7 with mRNA levels reduced by 60% and 26%, respectively (Fig. 2d), and human ATXN2 was not detected in cerebellar lysates from treated mice by Western blotting (Fig. 2e, f). Ten weeks after ICV injection, significant improvement in motor behavior compared to saline-ICV injected mice was seen (Fig. 1b). However, the rotarod performance of the ASO7 treated mice did not perfectly mirror that of wildtype mice. This might indicate that additional treatment time would be necessary to more completely restore cerebellar function. Rotarod results observed were not impacted by different mouse weights between the experimental groups (Extended Data Fig. 4).

Previously, we established transcriptome and protein profiles characterized by progressive changes in the course of degeneration in both mouse models[3]. To evaluate the effect of ASO7 on steady-state mRNA and protein levels we chose the top 6 mRNAs that showed the most significant changes in both mouse models[3]. Given that the ATXN2-Q127 model expresses the transgene specifically in PCs, we investigated genes significantly altered by SCA2 progression that are highly and specifically expressed in PCs: *Rgs8*, *Pcp2*, *Pcp4*, *Cep76*, *Homer3* and *Fam107b*[3]. RGS proteins inhibit mGlur1[10], which is a positive regulator of Ca^{2+} release from internal stores[11]. Because mGlur1 signaling is disrupted in SCA2 PCs leading to abnormal Ca^{2+} release, mGlur1 regulation may also be a function of Rgs8[3,12]. mGlur1 is also regulated in PCs by Homer3[13]. Pcp2 is a regulator of G(i/o)-coupled receptors including the P-type Ca^{2+} channel, important for sensorimotor control[14]. Pcp4 loss causes abnormal PC parallel fiber synapses[15], and Cep76 is required for normal centriole function[16]. *Fam107b* and *Rgs8* were identified as cerebellar hub genes with reduced expression in SCA1 mice[17]. Although significant increases at the mRNA level occurred for half of the genes after ASO7 treatment, we observed restored protein expression for all six of the genes on Western blots (Fig. 2, uncropped Western blots in Supplemental Fig. 1). This observation is consistent with an emerging role of polyglutamine expanded ATXN2 in translational dysregulation[3,18].

PCs are spontaneously firing neurons with a resting firing frequency of 40–50 *Hz* in mammals. The circuits underlying cerebellar learning and functioning are well understood[12,19,20] with PCs integrating signals received from parallel and climbing fibers and providing the only output from cerebellar cortex to deep cerebellar nuclei (DCN). In acute slice preparations, we had previously shown that mutant *ATXN2* caused a slowing of PC firing. This change had an onset and progression that closely mirrored that of motor deficits with onset at 6–8 weeks and an eventual slowing to 20 *Hz* at 24 weeks of age[4]. It has been suggested that the change in PC physiology is tightly linked to Ca^{2+} homeostasis and subsequent cell death[12,21]. This tight linkage between behavior and physiology led us to hypothesize that ASO treatment would restore normal PC firing. We injected ATXN2-Q127 mice at 8 wks and analyzed PC physiology 6 and 14 wks later in acute cerebellar slices. Similarly, we injected BAC-Q72 mice at 30 wks, >12 weeks after motor phenotype onset, and analyzed PC firing 10 wks later. In both models, a single injection of ASO7 resulted in near complete restoration of normal PC firing frequency (Figs. 3–4). Mice in these experiments were subsets of those in Figs. 1a and b with established rotarod phenotypes. These results suggest that *ATXN2* ASO treatment directly affects PC physiology and at least in part explains the amelioration of motor behavior.

SCA2 and other polyglutamine diseases are characterized by toxic gains of function, suggesting that therapeutics that lower expression of the disease causing genes would be beneficial. ASOs represent an ideal approach for directly lowering *ATXN2* expression because ASOs are sequence-specific, well tolerated, can reach CNS targets by intrathecal delivery. Feasibility is further supported by an early-phase human clinical trial to develop an ASO therapy for SOD1-ALS[22], and most recently by the FDA approval of the ASO drug nusinersin for spinal muscular atrophy (SMA). Various approaches to ASO therapeutics for polyglutamine diseases have been developed including targeting wildtype and mutant alleles as in this study or attempting to target mutant alleles via the expanded CAG repeat or via SNPs in linkage disequilibrium with the mutation[23,24]. DCN injected adeno-associated viruses (AAVs) targeting shRNAs to PCs were also effective for SCA1, reducing target expression and improving motor and cerebellar phenotypes in SCA1 transgenic mice[25,26]. At least for SCA2 and with the caveats of preclinical mouse studies, the strategy of targeting both mutant and WT alleles is showing promise. One potential advantage of ASOs over current viral vectors is that they distribute through the nervous system whereas adenoviral vectors are primarily transported transynaptically (also, gene transfer comes with more complex safety concerns). Thus for SCA2, AAVs injected into DCN neurons would reach PCs, but may not reach other neuronal groups.

In conclusion, we rigorously screened ASOs to identify a potent and well tolerated ASO, ASO7, that lowered cerebellar *ATXN2* expression, and verified in two SCA2 models that ASO7 delayed SCA2 motor and electrophysiological phenotypes in replicate experiments. Cerebellar degenerative diseases provide excellent model systems to study the interaction of dysfunction in a neuronal network, behavior and neurodegeneration. Our studies suggest that reduction of mutant ATXN2 effects all three domains including endophenotypic markers of cell death common in ataxias[3,17,27]. Multiple lines of evidence suggest that ASOs may have applications in human patients. ASO7 lowered expression of wildtype and mutant ATXN2 in SCA2 patient-derived fibroblasts (Extended Data Fig. 5). ASO7 delivered by ICV injection

localized throughout the spinal column and lowered *ATXN2* expression not only in brain, but also in spinal cord (data not shown). Notably, lowering of *ATXN2* by ASO treatment or genetic knockout delays dysfunction and greatly extends survival[28]. ASO7 or ASOs with further modifications in ASO chemistry may provide an effective human drug for SCA2, ALS caused by *ATXN2* mutation and other forms of ALS.

ONLINE METHODS

SCA2 mice

Pcp2-ATXN2-Q127 (ATXN2-Q127) transgenic mice express the full-length human *ATXN2*-$[CAG]_{127}$ cDNA under the control of the mouse Purkinje cell protein 2 (L7) promoter (*Pcp2*). ATXN2-Q127 mice in this study had a B6;D2 hybrid background. ATXN2-Q127 mice are described in Hansen et al., 2013 and Dansithong et al., 2015[29,30]. BAC-ATXN2-Q72 (BAC-Q72) mice were created using a contiguous 169 kb human *ATXN2* gene sequence including 16 kb upstream *ATXN2* sequence, the entire *ATXN2*-$[CAG]_{72}$ coding region (with introns) and 3 kb of *ATXN2* 3'-UTR and downstream sequence. BAC-Q22 are identical to BAC-Q72 but with the normal length CAG repeat. BAC-Q72 and BAC-Q72 mice used in this study had a FVB;B6 hybrid background. Creation of BAC-Q72 and BAC-Q22 mice is described in Dansithong et al., 2015[29]. BAC-Q22 mice were used in some *in vivo* ASO testing experiments that are not shown. Animals were genotyped by two separate PCR reactions using SCA2A/SCA2B and BM13-F/BM14-R genotyping primers (Supplementary Table 2). All animal work was done under an approved IACUC protocols at the University of Utah and University of California Los Angeles. One week post-surgery animals were recombined into cages of four mice for the duration of the study. To ensure blinding, ASO treated and saline treated mice were housed together and the technician performing behavioral testing was not aware of treatment status. Comments on study rigor including blinding are provided in Supplemental Discussion.

Antisense Oligonucleotides

All antisense oligonucleotides were 20 bp in length, included five 2'-*O*-methoxyethyl (MOE) modified nucleotides at each end of the oligonucleotide, with ten DNA nucleotides in the center, and were phosphorothioate modified in all positions. ASOs were synthesized as previously described[31]. The program Bowtie[32] was used to determine the predicted off-targets for the *ATXN2* ASOs in the mouse transcriptome (pre- and m-RNA). This analysis confirmed that the *ATXN2* ASOs do not bind any RNA other than *ATXN2* with full complementarity. We further verified that none of the lead ASOs had sequences that would target the closely homologous *ATXN2L* gene.

ICV ASO Injections

ASOs were delivered to mice by intracerebroventricular (ICV) injection. Injection were made using a Hamilton 26s gauge needle. For mice in Figs 1–4 injections were 6 μl of 35 μg/μl ASO7 diluted in normal saline for a total of 210 μg. Control mice received the same volume of normal saline. For other mice in Extended Data Figures injection volumes varied from 6–10 μl to deliver the indicated ASO concentrations, with ASOs diluted accordingly with normal saline. Injections were made under anesthesia with a mixture of oxygen and

isoflurane, using a Stoelting stereotaxic frame. Anesthesia was initiated using 3% isoflurane for 5 min and the isoflurane mixture was lowered to 2% during injections. Stereotaxic bregma coordinates were −0.46 mm anteroposterior, −1.0 mm lateral (right side); −2.5 mm dorsoventral. Needles were removed 4 min after ASO delivery. Mice were maintained on a 39°C isothermal pad while anesthesized and during recovery.

Cell culture

SCA2 patient-derived skin fibroblasts (SCA2-CAG35) were cultured and maintained in DMEM medium supplemented with 10% fetal bovine serum, penicillin and streptomycin. All subjects gave written consent and the studies were approved by the Institutional Review Board at the University of Utah. ASO transfections were performed by electroporation of,one million cells with 0, 0.35, 1 or 2 μM ASO7 using the Neon transfection system (Invitrogen Inc., USA) according to manufacturer's protocol, followed by plating in 6 well plates.. The cells were harvested at 5 days post-electroporation for analyses.

Western blot analyses

Protein extracts were prepared by homogenization of mouse cerebella in extraction buffer (25 mM Tris-HCl pH 7.6, 300 mM NaCl, 0.5% Nonidet P-40, 2 mM EDTA, 2 mM $MgCl_2$, 0.5 M urea and protease inhibitors; Sigma; cat# P-8340) followed by centrifugation at 4°C for 20 min at 16,100 × g. Only supernatants were used for Western blotting to determine the steady-state levels of proteins using the antibodies listed below. Protein extracts were resolved by SDS-PAGE and transferred to Hybond P membranes (Amersham Bioscience Inc., USA). After blocking with 5% skim milk in 0.1% Tween 20/PBS, the membranes were incubated with primary antibodies in 5% skim milk in 0.1% Tween 20/PBS for 2 hrs at room temperature or overnight at 4°C. After washing in 0.1% Tween 20/PBS, the membranes were incubated with the corresponding secondary antibodies conjugated with HRP in 5% skim milk in 0.1% Tween 20/PBS for 2 hrs at room temperature and washed again. Signals were detected by using the Immobilon Western Chemiluminescent HRP Substrate (Millipore Inc., USA; cat# WBKLSO100) according to the manufacturer's protocol. The intensity of proteins was determined using the ImageJ software analysis system and proteins were quantitated as a ratio to β-Actin.

Immunohistochemical (IHC) staining

Excised tissues were fixed in 4% paraformaldehyde for 72 h, then were treated in 75% ethanol for 24 hrs, after which paraffin embedding was performed by automated instrumentation (University of Utah Histology Core). Embedded tissues were sectioned in 4 μm sections on a Leica microtome and mounted on glass slides. Sections were then deparaffinized and rehydrated (2 washes in xylene, 2 washes in 100% ethanol, 2 washes in 95% ethanol, 1 wash in water). Endogenous peroxidases were quenched by treating in 3% H_2O_2 in methanol for 10 min followed by 2 washes in 1x wash buffer (TA-999-TT Fisher Scientific). Sections were treated with Proteinase K for 10 min (Dako cat#S3020) then washed 2 times. Sections were then treated with Cyto-Q Background Buster (Innovex Biosciences) then washed 2 times. Primary rabbit anti-ASO antibody (Ionis Pharmaceuticals) diluted 1:40,000 in antibody diluent (2% BSA, 5% normal donkey serum, in 1x Wash Buffer) was then incubated in on sections overnight at 4°C. Sections were then

washed 3 times and incubated in secondary donkey anti-rabbit-HRP antibody (Jackson ImmunoResearch) 1:200 in antibody diluent for 30 min at room temperature, followed by 3 washes in wash buffer. Antibody detection was accomplished using DAB Chromagen (DAKO) followed by 2 washes in wash buffer. Sections were counterstainined using hematoxylin (Fisher), washed 2 times in water, dipped in an acid-ethanol decolorizing solution (500 μl HCI to 200 ml of 70% ethanol), and washed in water. Sections were then dehydrated (2 washes in 95% ethanol, 2 washes in 100% ethanol, 2 washes in xylene) and mounded using permamount (Fisher). Peroxidase staining was imaged on an EVOS FL Microscope using 2x, 10x, and 40x objectives.

Antibodies

The following antibodies were used for western blotting: ATXN2 mAb (1: 4000) (BD Biosciences Inc., 611378), 5TF1–1C2 mAb (1:3000) (Millipore Inc., MAB1574), RGS8 rabbit polyclonal Ab (1:5000) (Novus Biologicals, NBP2–20153), PCP-2 antibody (F-3) (1: 3000) (Santa Cruz Inc., sc-137064), β-Actin mAb HRP conjugated (1:10,000) (Sigma Inc., A3854). Anti-PCP4 antibody (1: 5000) (Abcam, ab197377), Homer-3 antibody (E-6) (1: 2000) (Santa Cruz Inc., sc-376155), CEP76 antibody (1: 5000) (Novus biologicals, NBP1–28749), Anti-FAM107B antibody (1: 5000) (Abcam, ab175148). The secondary antibodies were goat anti-mouse IgG-HRP antibody (1:5000) (Sigma Inc., A2304) and goat anti-rabbit IgG-HRP antibody (1:5000) (Vector laboratories, PI-1000). Anti-ASO antibody (Ionis Pharmaceuticals) and appropriate secondary antibody used for IHC are described in the previous paragraph.

Quantitative PCR

Total RNA was extracted from cerebellar tissues, spinal cord tissues or SCA2-CAG35 patient fibroblasts using the RNeasyMini Kit (Qiagen Inc., USA) according to the manufacturer's protocol. DNAse I treated RNAs were used to synthesize cDNAs using the ProtoScript cDNA First Strand cDNA Synthesis Kit (New England Biolabs Inc., USA). Primers for RT-PCR were designed to prevent amplification from genomic DNA (annealing sites in different exons or across intron-exon boundaries). PCR primers sequences are provided in Supplementary Table 2. Quantitative RT-PCR was performed in Bio-Rad CFX96 (Bio-Rad Inc., USA) with the Power SYBR Green PCRMasterMix (Applied Biosystems Inc, USA). PCR reaction mixtures contained SYBR Green PCRMasterMix and 0.5 pmol primers and PCR amplification was carried out for 45 cycles: denaturation at 95 °C for 10 sec, annealing at 60 °C for 10 sec and extension at 72 °C for 40 sec. The threshold cycle for each sample was chosen from the linear range and converted to a starting quantity by interpolation from a standard curve run on the same plate for each set of primers. Gene expression levels were normalized to the *GAPDH* or *Actin* mRNA levels.

Rotarod Testing

Cohorts of mice were bred from randomly selected breeding animals. Cohorts were selected randomly to have a balanced number of males and females. Rotarod groups were controlled for baseline rotarod performance as well as weight (treatment groups within any experiment had the same average rotarod latency to fall and weight before treatments). Rotarod testing was performed on the Rotamex-5 instrument (Columbus Instruments, Columbus OH). When

performing tests, animals were taken to a separate testing room and habituated there for at least an hour before testing. Animals were tested in the same order, and beginning at the same time each day (1 p.m.). Mice in different treatment groups were housed together and the technician was blinded to treatment status. All rotarod testing in this study was performed by the same technician. Rotarod values per each week of testing were collected over five days. On day 1 mice were handled for 2 minutes per mouse. On day 2 mice were introduced to the rotarod using the following paradigm: 4 RPM for 2 min, then increasing by 1 RPM per every 15 s to 10 RPM for 60 s. Tests on days 3–5 on the accelerating rotarod were identical with three tests per day as follows: Mice were placed on the rod which from 0 RPM accelerated 1 RPM every 9 s until mice fell from the rod. Most mice fell before 40 RPM (6 min); all mice fell before 50 RPM (7.5 min). Values of latency to fall in seconds were recorded. The rotarod was cleaned between individual tests. No animals were disqualified from testing once testing had begun, either during training or testing phases.

Electrophysiology

The preparation of parasagittal cerebellar slices closely followed our previously published description of the process[33]. Cerebella from BAC-Q72, ATXN2-Q127 and their age-matched WT littermates were removed and quickly immersed in 4 °C extracellular solution bubbled with 95% O_2 and 5% CO_2 (119 mM NaCl, 26 mM $NaHCO_3$, 11 mM glucose, 2.5 mM KCl, 2.5 mM $CaCl_2$, 1.3 $MgCl_2$ and 1 mM NaH_2PO_4, pH 7.4 when gassed with 5% CO_2 / 95% O_2). Parasagittal cerebellar slices (285 μm) were sectioned using a vibratome (Leica VT1000). Extracellular recordings were acquired in voltage-clamp mode at near physiological temperature (34.5 ± 1°C) using a dual channel heater controller (Model TC-344B, Warner Instruments) and constantly perfused with carbogen-bubbled extracellular solution at a rate of 3 ml per min. Cells were visualized on an upright microscope (Leica) with a 40x water-immersion lens. Borosilicate glass pipettes with resistances between with 1 to 3 MΩ were filled with extracellular solution and used for recording action potential-associated capacitative current transients. The pipette potential was held at 0 mV and placed close to the Purkinje neuron axon hillock (soma/axon). Data were acquired at 20 kHz using a Multiclamp 700b amplifier, Digidata 1440 with pClamp10 (Molecular Devices) and filtered at 4 kHz. Each Purkinje neuron recording spanned a duration of 2 minutes and a total of 40 to >100 cells were measured from each mouse. A total of 1 to 4 mice per genotype were used and the experimenter was blinded to the mouse genotype. Experiments were analyzed using both Clampfit and Igor Program and further analyzed using Microsoft Excel. Figures were made using Igor. Results are presented as mean ±SEM.

Statistical Analysis

Statistical differences between selected groups evaluated by qPCR were determined by two-tailed Student's *t*-tests. Electrophysiological data were also evaluated using analysis of variance (ANOVA) tests followed by post-hoc tests of significance (Tukey's multiple comparison test). Statistical comparisons of rotarod data were determined using the method of generalized estimating equations (GEE) with the independent correlation option using Stata 12 (procedures xtset followed by xtgee). The independent correlation option was employed because in the three day rotarod paradigm, regressions for wildtype mice

frequently have more positive correlation coefficients than SCA2 mice. Regression analyses were performed using GraphPad Prism.

Data Availability

All data generated or analysed during this study are included in this published article (and its supplementary information files).

Extended Data

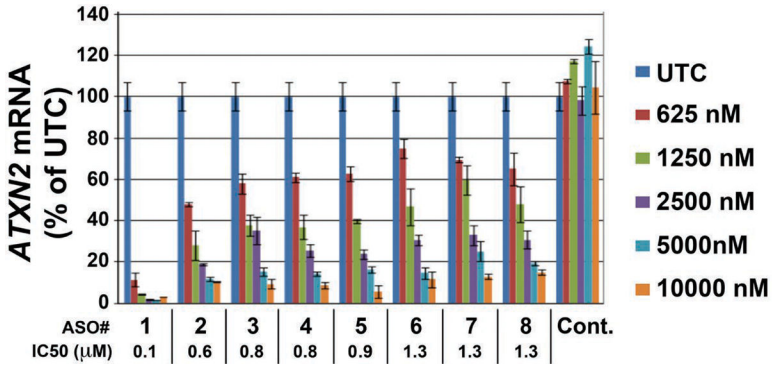

Extended Data Figure 1.

In vitro screen for *ATXN2* ASOs by qPCR. A total of 152 ASOs were delivered at 4.5 μM to HepG2 cells by electroporation in two 384-well plates. *ATXN2* expression was evaluated by qPCR (n=3 wells per ASO). Shown is the evaluation of the eight best positive hit ASOs for IC50 determination. Values are means ± SD of *ATXN2* quantity relative to total RNA. Cont. = scrambled control ASO.

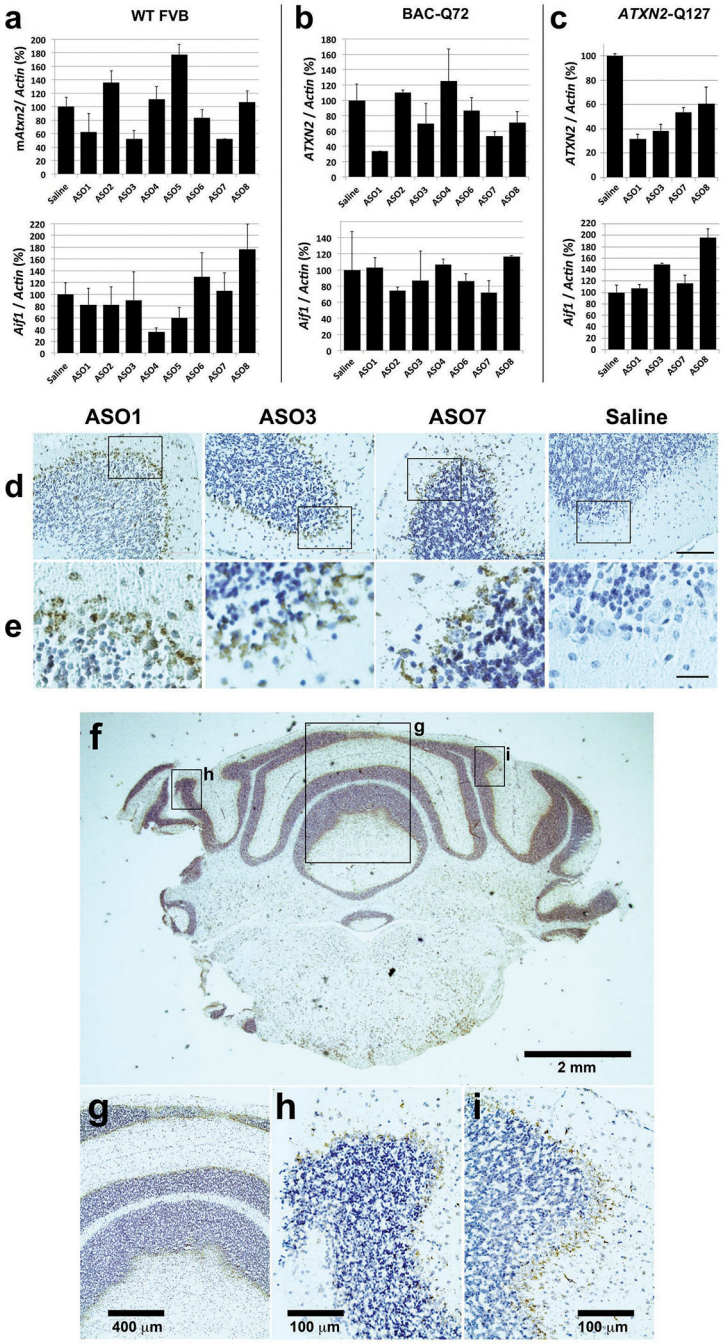

Extended Data Figure 2.

Positive hit ASOs evaluated *in vivo.* **a-c,** 250 µg of the indicated ASOs in a total of 7 µl was delivered by ICV injection. After 7 days treatment the expression of mouse *Atxn2* or human *ATXN2* and *Aif1* was determined by qPCR relative to actin. **a,** Wildtype FVB mice. **b,** BAC-Q72 mice. **c,** ATXN2-Q127 mice. Values are means ± SD relative to those determined from normal saline treated mice. The n number of mice (left-to-right in each chart) was as follows: a, 2,2,2,3,2,2,2,2,1. b, 2,1,1,2,2,2,1,2. c, 2,3,1,1,1. **d & e,** ASOs localized to the cerebellar Purkinje cell layer of treated mice. Mice were treated by ICV injection into the

right lateral ventricle of the indicated lead ASOs for 7 days in BAC-Q72 mice (ASO3 and ASO7 used at 250 μg) or 10 wks in ATXN2-Q127 mice (ASO1 used at 200 μg). ASOs were localized in paraffin embedded sections by immunohistochemical peroxidase staining using anti-ASO antibody. Saline= ATXN2-Q127 mice treated by ICV injection of 7 μl saline for 10 wks. **d,** 10x objective. **e,** 3x digital zoom of a region of the PC layer in the corresponding 10x image, indicated by the box. Bar = 100 μm (**d**), 25 μm (**e**). **f-i,** Distribution of ASO7 in the cerebellum. **f,** ASO7 was distributed in Purkinje cell layers throughout the cerebellum (2x objective). Higher power images at regions indicated in **f** demonstrated ASO7 localization in Purkinje cells across the cerebellum: **g,** 10x objective; **h & i,** 40x objective.

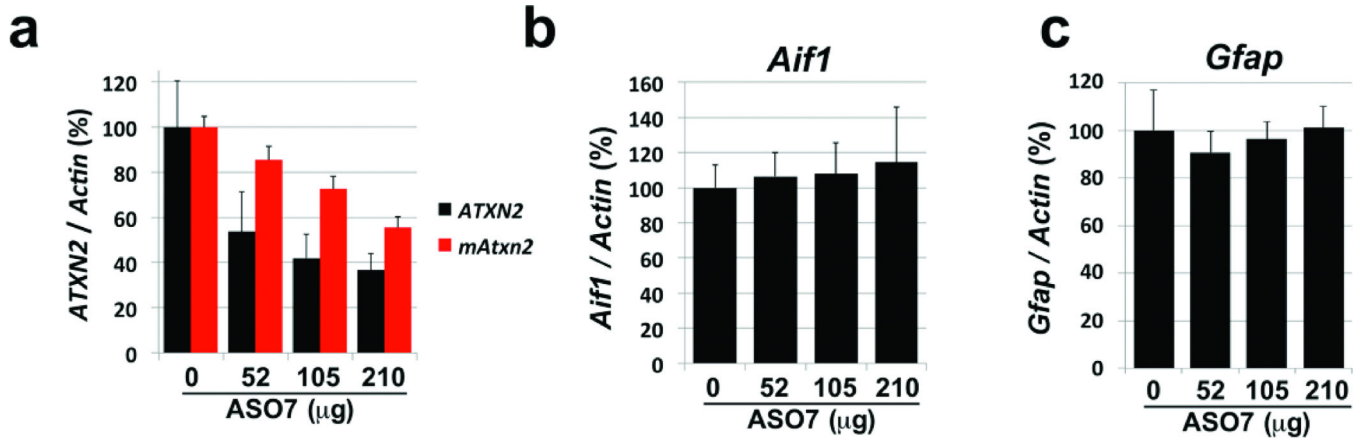

Extended Data Figure 3.

Effects of ASO7 on *ATXN2* expression *in vivo* by dose and time. **a-c**, Dosewise effect of ASO7 on *ATXN2* expression in BAC-Q72 mice treated with ASO7 by ICV injection for 14 days. **a**, Expression of cerebellar human *ATXN2* and mouse *Atxn2* determined by qPCR. **b**, Cerebellar *Aif1* expression determined by qPCR. **c**, Cerebellar *Gfap* expression determined by qPCR. The n # of mice for the saline, 52 μg, 105 μg, and 210 μg treatments was 3, 2, 3 and 3, respectively.

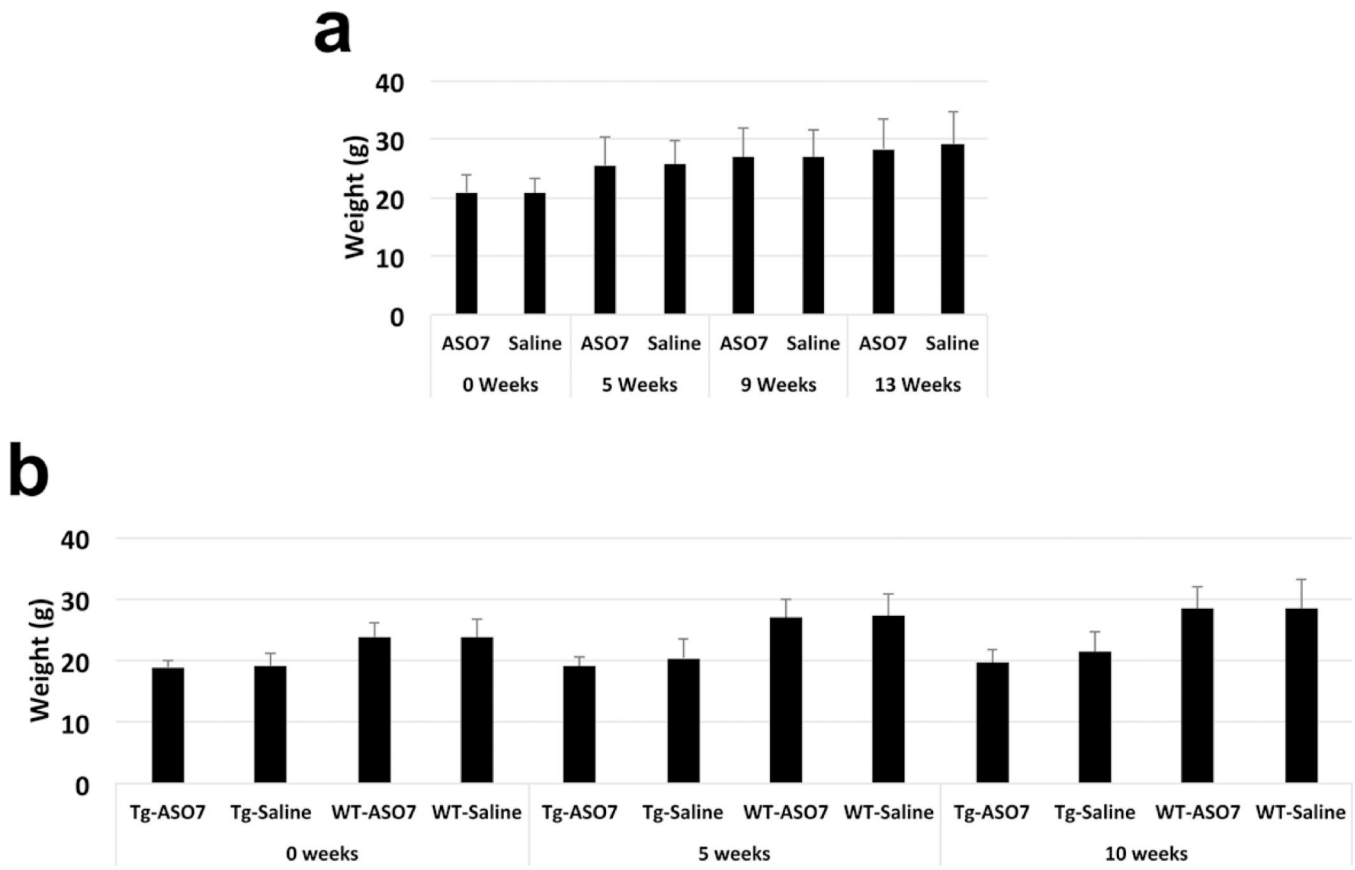

Extended Data Figure 4.

Weights of mice before and after rotarod testing. **a**, Rotarod test of ATXN2-Q127 mice treated with a single ICV dose of 210 μg ASO7. **b**, Rotarod test of BAC-Q72 mice treated with a single ICV dose of 175 μg ASO7. Weeks of ASO treatments are indicated on the X-axes. Significance tests demonstrated significant differences between weights of BAC-Q72 mice compared to wildtype littermates ($p<0.001$ for any age group, Student's t-test). Comments on the relevance of mouse weights on motor phenotype testing are provided in Supplementary Discussion.

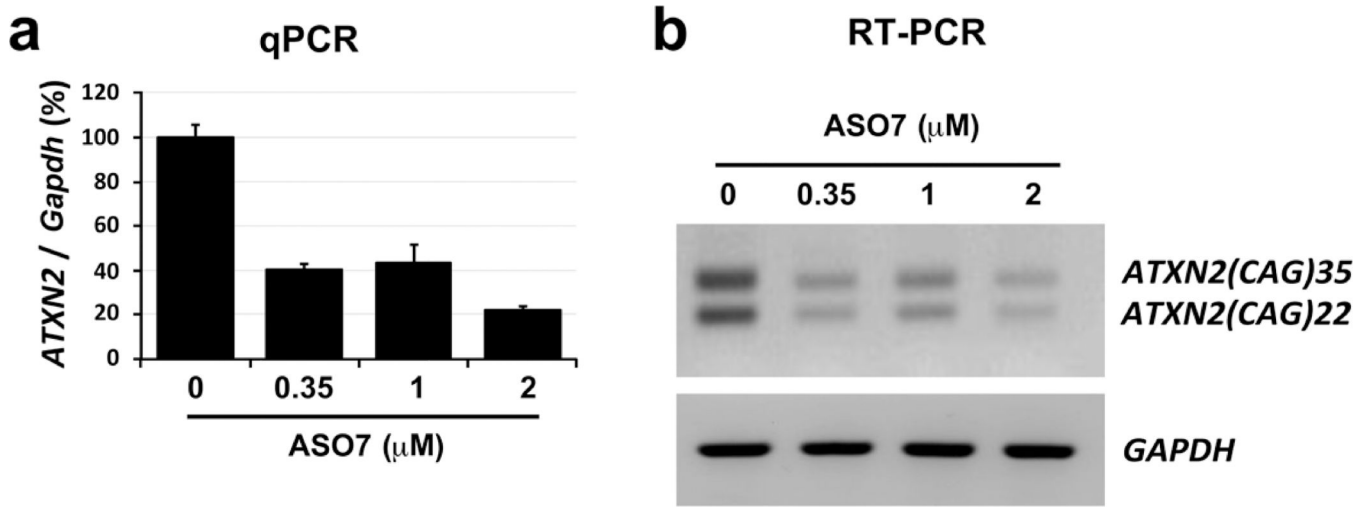

Extended Data Figure 5.

ASO7 lowered expression of wildtype and mutant *ATXN2* in cultured SCA2 patient derived fibroblasts. **a**, Patient derived SCA2(CAG35) fibroblasts were transfected with the indicated quantities of ASO7. After 72 hours RNAs were prepared and total *ATXN2* expression was determined by qPCR. **b**, To determine ASO7 effect on the expression of non-mutant (CAG22) and mutant (CAG35) *ATXN2*, RT-PCR reactions were evaluated by agarose gel electrophoresis, with loading controlled by *GAPDH.*

Supplementary Material

Refer to Web version on PubMed Central for supplementary material.

Acknowledgements

We thank Paymaan Jafar-nejad for his contributions to interpreting results and for reading and editing the manuscript. We thank Lance Pflieger for contributing to the production of supplemental data. This work was supported by grants R01NS33123, R56NS33123 and R37NS033123 from the National Institutes of Neurological Disorders and Stroke (NINDS) to S.M.P., the Noorda foundation to S.M.P., NINDS grants RC4NS073009 and R21NS081182 to D.R.S. and S.M.P., NINDS grant NS090930 to T.S.O., and a gift from Ionis Pharmaceuticals. S.M.P. received grant support from the Target ALS Foundation.

References

1. Pulst SM, Nechiporuk A & Starkman S Anticipation in spinocerebellar ataxia type 2. Nat Genet 5, 8–10, doi:10.1038/ng0993-8c (1993).
2. Rigo F, Seth PP & Bennett CF Antisense oligonucleotide-based therapies for diseases caused by pre-mRNA processing defects. Adv. Exp. Med. Biol 825, 303–352, doi:10.1007/978-1-4939-1221-6_9 (2014). [PubMed: 25201110]
3. Dansithong W et al. Ataxin-2 regulates RGS8 translation in a new BAC-SCA2 transgenic mouse model. PLoS Genet 11, e1005182, doi:10.1371/journal.pgen.1005182 (2015). [PubMed: 25902068]
4. Hansen ST, Meera P, Otis TS & Pulst SM Changes in Purkinje cell firing and gene expression precede behavioral pathology in a mouse model of SCA2. Hum Mol Genet 22, 271–283, doi: 10.1093/hmg/dds427 (2013). [PubMed: 23087021]
5. Pulst SM Degenerative ataxias, from genes to therapies: The 2015 Cotzias Lecture. Neurology 86, 2284–2290, doi:10.1212/WNL.0000000000002777 (2016). [PubMed: 27298447]

6. Houlden H & Singleton AB The genetics and neuropathology of Parkinson's disease. Acta Neuropathol 124, 325–338, doi:10.1007/s00401-012-1013-5 (2012). [PubMed: 22806825]
7. Scoles DR et al. Repeat Associated Non-AUG Translation (RAN Translation) Dependent on Sequence Downstream of the ATXN2 CAG Repeat. PLoS One 10, e0128769, doi:10.1371/journal.pone.0128769 (2015). [PubMed: 26086378]
8. Huynh DP, Figueroa K, Hoang N & Pulst SM Nuclear localization or inclusion body formation of ataxin-2 are not necessary for SCA2 pathogenesis in mouse or human. Nat Genet 26, 44–50, doi:10.1038/79162 (2000). [PubMed: 10973246]
9. Huynh DP, Maalouf M, Silva AJ, Schweizer FE & Pulst SM Dissociated fear and spatial learning in mice with deficiency of ataxin-2. PLoS One 4, e6235, doi:10.1371/journal.pone.0006235 (2009). [PubMed: 19617910]
10. Saugstad JA, Marino MJ, Folk JA, Hepler JR & Conn PJ RGS4 inhibits signaling by group I metabotropic glutamate receptors. J Neurosci 18, 905–913 (1998). [PubMed: 9437012]
11. Abdul-Ghani MA, Valiante TA, Carlen PL & Pennefather PS Metabotropic glutamate receptors coupled to IP3 production mediate inhibition of IAHP in rat dentate granule neurons. J Neurophysiol 76, 2691–2700 (1996). [PubMed: 8899638]
12. Meera P, Pulst SM & Otis TS Cellular and circuit mechanisms underlying spinocerebellar ataxias. The Journal of physiology, doi:10.1113/JP271897 (2016).
13. Mizutani A, Kuroda Y, Futatsugi A, Furuichi T & Mikoshiba K Phosphorylation of Homer3 by calcium/calmodulin-dependent kinase II regulates a coupling state of its target molecules in Purkinje cells. J Neurosci 28, 5369–5382, doi:10.1523/JNEUROSCI.4738-07.2008 (2008). [PubMed: 18480293]
14. Iscru E et al. Sensorimotor enhancement in mouse mutants lacking the Purkinje cell-specific Gi/o modulator, Pcp2(L7). Mol. Cell. Neurosci 40, 62–75, doi:10.1016/j.mcn.2008.09.002 (2009). [PubMed: 18930827]
15. Wei P, Blundon JA, Rong Y, Zakharenko SS & Morgan JI Impaired locomotor learning and altered cerebellar synaptic plasticity in pep-19/PCP4-null mice. Mol Cell Biol 31, 2838–2844, doi:10.1128/MCB.05208-11 (2011). [PubMed: 21576365]
16. Tsang WY et al. Cep76, a centrosomal protein that specifically restrains centriole reduplication. Dev Cell 16, 649–660, doi:10.1016/j.devcel.2009.03.004 (2009). [PubMed: 19460342]
17. Ingram M et al. Cerebellar Transcriptome Profiles of ATXN1 Transgenic Mice Reveal SCA1 Disease Progression and Protection Pathways. Neuron 89, 1194–1207, doi:10.1016/j.neuron.2016.02.011 (2016). [PubMed: 26948890]
18. Fittschen M et al. Genetic ablation of ataxin-2 increases several global translation factors in their transcript abundance but decreases translation rate. Neurogenetics 16, 181–192, doi:10.1007/s10048-015-0441-5 (2015). [PubMed: 25721894]
19. Lee KH et al. Circuit mechanisms underlying motor memory formation in the cerebellum. Neuron 86, 529–540, doi:10.1016/j.neuron.2015.03.010 (2015). [PubMed: 25843404]
20. Lang EJ et al. The Roles of the Olivocerebellar Pathway in Motor Learning and Motor Control. A Consensus Paper. Cerebellum, doi:10.1007/s12311-016-0787-8 (2016).
21. Liu J et al. Deranged calcium signaling and neurodegeneration in spinocerebellar ataxia type 2. J Neurosci 29, 9148–9162, doi:29/29/9148 [pii] 10.1523/JNEUROSCI.0660-09.2009 (2009). [PubMed: 19625506]
22. Miller TM et al. An antisense oligonucleotide against SOD1 delivered intrathecally for patients with SOD1 familial amyotrophic lateral sclerosis: a phase 1, randomised, first-in-man study. Lancet Neurol 12, 435–442, doi:10.1016/S1474-4422(13)70061-9 (2013). [PubMed: 23541756]
23. Skotte NH et al. Allele-specific suppression of mutant huntingtin using antisense oligonucleotides: providing a therapeutic option for all Huntington disease patients. PLoS One 9, e107434, doi:10.1371/journal.pone.0107434 (2014). [PubMed: 25207939]
24. Carroll JB et al. Potent and selective antisense oligonucleotides targeting single-nucleotide polymorphisms in the Huntington disease gene / allele-specific silencing of mutant huntingtin. Molecular therapy : the journal of the American Society of Gene Therapy 19, 2178–2185, doi:10.1038/mt.2011.201 (2011). [PubMed: 21971427]

25. Xia H et al. RNAi suppresses polyglutamine-induced neurodegeneration in a model of spinocerebellar ataxia. Nat Med 10, 816–820, doi:10.1038/nm1076nm1076 [pii] (2004). [PubMed: 15235598]

26. Keiser MS, Boudreau RL & Davidson BL Broad Therapeutic Benefit After RNAi Expression Vector Delivery to Deep Cerebellar Nuclei: Implications for Spinocerebellar Ataxia Type 1 Therapy. Mol Ther, doi:10.1038/mt.2013.279 (2013).

27. Rodriguez-Lebron E, Liu G, Keiser M, Behlke MA & Davidson BL Altered Purkinje cell miRNA expression and SCA1 pathogenesis. Neurobiol Dis 54, 456–463, doi:10.1016/j.nbd.2013.01.019 (2013). [PubMed: 23376683]

28. Becker LA et al. Therapeutic reduction of ataxin 2 extends lifespan and rescues pathological features of ALS in TDP-43 transgenic mice. Nature XXXXX (2017).

29. Dansithong W et al. Ataxin-2 regulates RGS8 translation in a new BAC-SCA2 transgenic mouse model. PLoS Genet 11, e1005182, doi:10.1371/journal.pgen.1005182 (2015). [PubMed: 25902068]

30. Hansen ST, Meera P, Otis TS & Pulst SM Changes in Purkinje cell firing and gene expression precede behavioral pathology in a mouse model of SCA2. Hum Mol Genet 22, 271–283, doi:10.1093/hmg/dds427 (2013). [PubMed: 23087021]

31. Swayze EE et al. Antisense oligonucleotides containing locked nucleic acid improve potency but cause significant hepatotoxicity in animals. Nucleic Acids Res. 35, 687–700, doi:10.1093/nar/gkl1071 (2007). [PubMed: 17182632]

32. Langmead B, Trapnell C, Pop M & Salzberg SL Ultrafast and memory-efficient alignment of short DNA sequences to the human genome. Genome Biol 10, R25, doi:10.1186/gb-2009-10-3-r25 (2009). [PubMed: 19261174]

33. Meera P, Wallner M & Otis TS Molecular basis for the high THIP/gaboxadol sensitivity of extrasynaptic GABA(A) receptors. J Neurophysiol 106, 2057–2064, doi:10.1152/jn.00450.2011 (2011). [PubMed: 21795619]

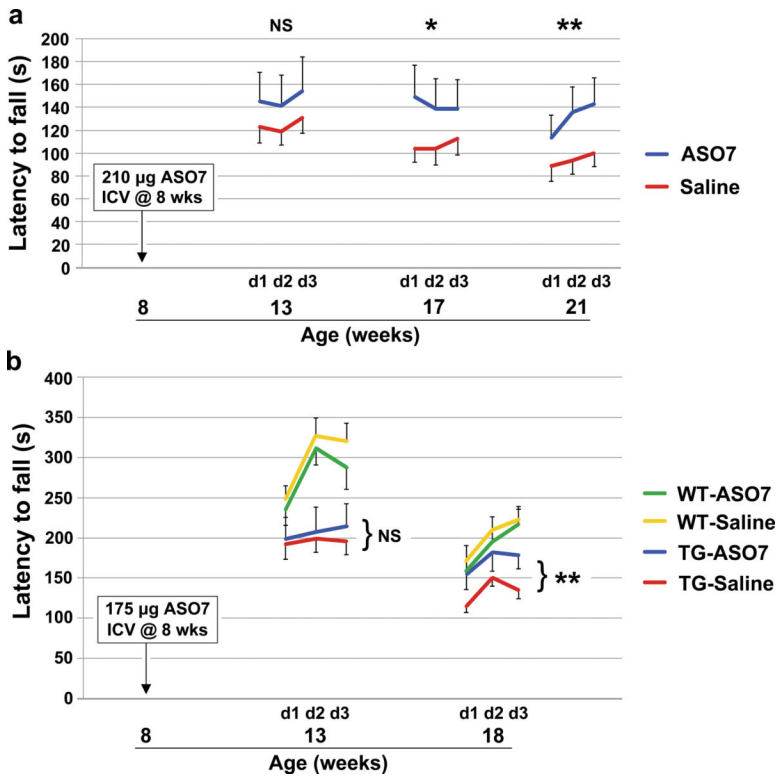

Figure 1.

Effect of ASO7 on motor phenotypes. **a**, Eight wk old ATXN2-Q127 mice were treated with 210 µg ASO7 or saline ICV and rotorod tested at the indicated ages. n=15 mice per group. **b**, Eight wk old BAC-Q72 mice and wildtype littermates were treated with 175 µg ASO7 or saline ICV and rotarod tested at the indicated ages. n= 13, 13, 11, 14 for WT-ASO, WT-Saline, TG-ASO, and TG-Saline, respectively. Values shown are mean±SE. Probabilities of significance were determined using the method of generalized estimating equations (GEE). NS, nonsignificant, *=$p<0.05$, **=$p<0.01$.

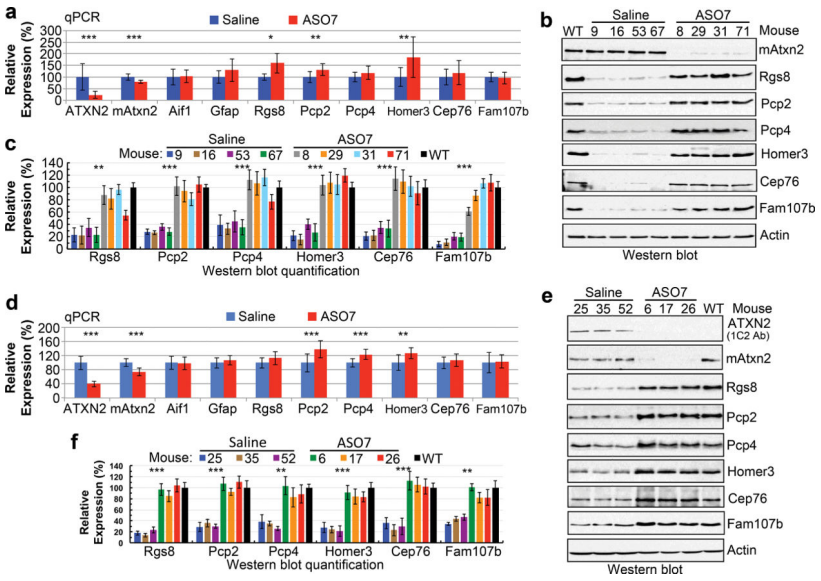

Figure 2.

Cerebellar gene expression for ASO treated SCA2 mice following rotatod tests. **a-c,** Expression in ATXN2-Q127 mice. **a**, ATXN2-Q127 mice were treated as in Fig. 1a and the cerebellar expression of the indicated genes was determined at 22 wks of age. The n number of mice for saline and ASO7 treatments, respectively, were: *ATXN2*, 11, 11; *Atxn2*, 11, 11; *Aif1*, 7, 8; *Gfap*, 11, 11; *Rgs8*, 4, 4; *Pcp2*, 11, 11; *Pcp4*, 10, 11; *Cep76*, 10, 11; *Homer3*, 10, 11; *Fam107b*, 10, 10. **b & c**, Cerebellar expression in ATXN2-Q127 mice for ATXN2, mouse Atxn2, Rgs8, Pcp2, Pcp4, Cep76, Homer3, Fam107b, and Actin (**b**), with abundances expressed as a percent relative to actin, determined densitometrically (**c**). **d-f,** Expression in BAC-Q72 mice. **d,** BAC-Q72 mice were treated as in Fig. 1b and the cerebellar expression of the indicated genes was determined at 19 wks of age. The n per group in qPCR analyses was 14 saline treated mice and 11 ASO7 treated mice for all genes except Rgs8 and Fam107b where the n was 14 saline treated and 10 ASO treated mice. Values are mean±SD. NS, nonsignificant, *=p<0.05, **=p<0.01, ***=p<0.001 by Student's t-test. **e**, Cerebellar expression in BAC-Q72 mice of expanded ATXN2 detected with anti-1C2 antibody, and expression of mouse Atxn2, Rgs8, Pcp2, Pcp4, Cep76, Homer3, Fam107b and Actin (**e**), with abundances expressed as a percent relative to actin, determined densitometrically (**f**). Values shown in **c** and **f** are mean±SD from three replicate blots.

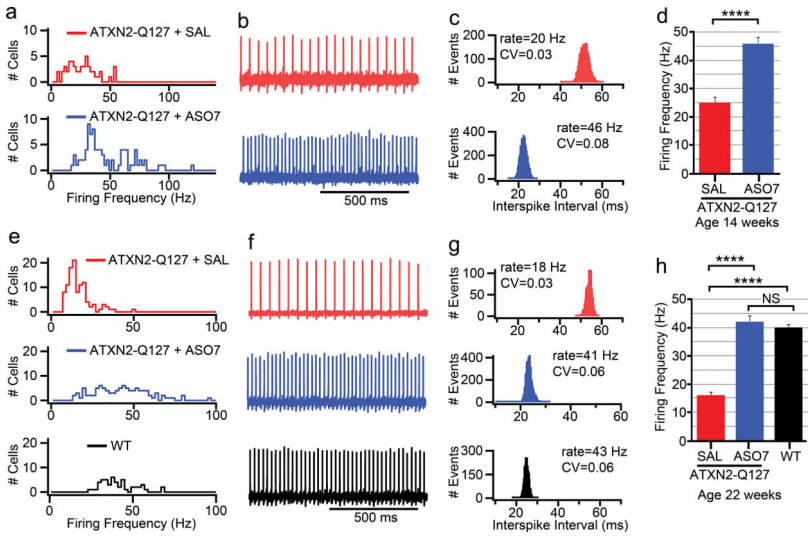

Figure 3.

Slow ATXN2-Q127 mouse PC firing frequency (FF) was restored by ASO7. **a-d**, ATXN2-Q127 mice were treated with 210 μg ASO7 or saline by ICV injection at 8 wks, and PC FF was evaluated at 14 wks of age. **a**, Mean FF distribution for PCs from saline and ASO7 treated mice. **b**, Representative PC traces of 1s duration, and (**c**) interspike-interval histogram of the same cell as in (**b**) calculated from 2 min duration, with coefficients of variation (CV) shown. **d**, Mean FF (±SEM) were 25±2 Hz for the saline treated mouse (n=50 neurons, mice=1) and 46±2 Hz for the ASO7 treated mice (n=88 neurons, mice=2) (****, $p<0.0001$, Student's t-test). **e-h**, ATXN2-Q127 mice were treated with 210 μg ASO7 or saline by ICV injection at 8 wks. PC FF was evaluated at 22 weeks of age. **e**, Mean FFs of all PCs measured from saline and ASO7 treated mice and age-matched WT mice. **f**, Representative PC traces of 1s duration, and (**g**) interspike-interval histogram of the same cell as in (**f**) calculated from 2 min duration, with CV values shown. **h**, Mean FF (± SEM) were 16±1 Hz for the saline treated ATXN2-Q127 mice (n=107 neurons, mice=2), 42±2 Hz for the ASO7 treated ATXN2-Q127 mice (n=102 neurons, mice=2), and 40±1 Hz for an age-matched WT mouse (n=50 neurons, mice=1). (****, $p<0.0001$, Student's t-test). All recordings were measured at 34.5±1 °C.

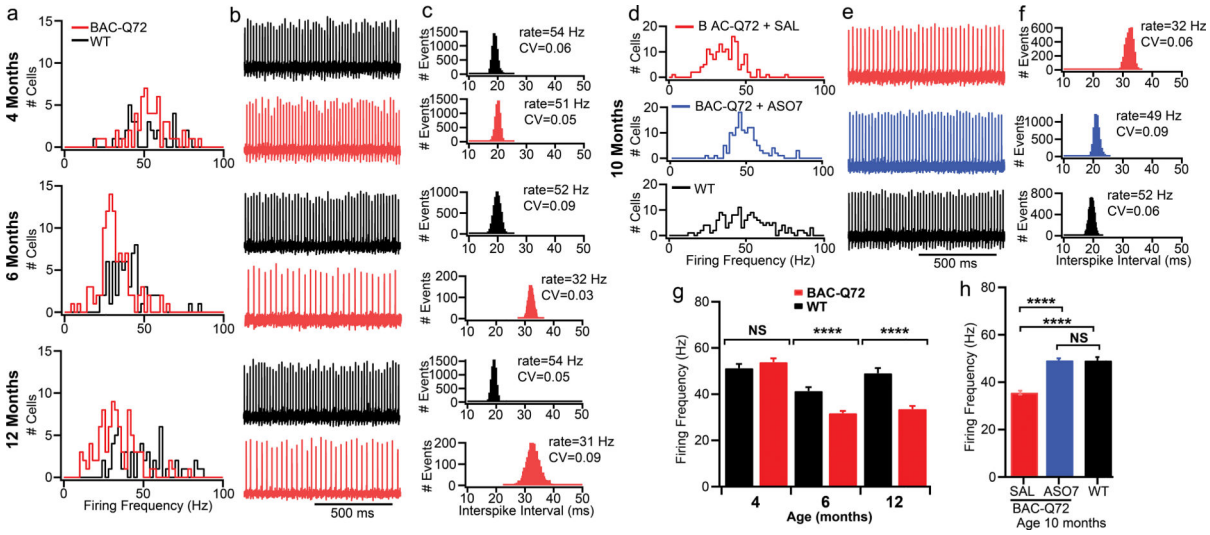

Figure 4.

Slow BAC-Q72 mouse PC FF was restored by ASO7. **a-c**, FFs of BAC-Q72 mice at indicated ages. **a**, FF distributions for WT and BAC-Q72 PCs. The n number of PCs were 33 WT, 59 BAC-Q72 (4 mo); 49 WT, 101 BAC-Q72 (6 mo); 55 WT, 92 BAC-Q72 (12 mo). **b**, Example recordings from PCs for WT and BAC-Q72 mice. **c**, Interspike intervals of the same cell over 2 min with mean FF and CV indicated. **d-f**, The PC FF was restored in 10 mo. old BAC-Q72 mice treated with 210 μg ASO7 ICV for 10 wks. **d**, PC FF in BAC-Q72 mice, BAC-Q72 mice treated with ASO7, and WT littermates. **e**, Representative PC 1s trace and (**f**) interspike intervals of the same cell over 2 min in saline treated BAC-Q72 mice, ASO treated BAC-Q72, and WT littermates with PC FF and CV indicated. **g-h**, Mean PC FFs in (**a**) and (**d**). **g**, Age-dependent PC FF in BAC-Q72 mice. At age 4 mo the mean FFs in Hz were 51±2 for WT (n=33 PCs, mice=1) and 54±2 for BAC-Q72 (n= 59 PCs, mice=1). At 6 mo the values were 41±2 for WT (n=49 PCs, mice=2) and 32±1 for BAC-Q72 (n=101 PCs, mice=2). At age 12 mo they were 49±2 for WT (n=55 PCs, mice=1) and 34±1 for BAC-Q72 (n=92 PCs, n=1). **h**, ASO7 treatment restored the PC FF of BAC-Q72 mice. The mean PC FF for 10 mo old BAC-Q72 mice treated with saline was 36±1 Hz (n=148 PCs, mice=3) while the mean FF of BAC-Q72 mice treated with ASO7 was 49±1 (n=134 PCs, mice=4), similar to that of WT mice (49±1, n=155 PCs, mice=3). (****, $p<0.0001$, ANOVA followed by Tukey's multiple comparison posthoc testing).